

The FinO Repressor of Bacterial Conjugation Contains Two RNA Binding Regions[†]Alexandru F. Ghetu,[‡] Michael J. Gubbins,[§] Kimio Oikawa,[‡] Cyril M. Kay,[‡] Laura S. Frost,[§] and J. N. Mark Glover^{*,‡}*Department of Biochemistry, University of Alberta, Edmonton, Alberta, T6G 2H7, Canada, and Department of Biological Sciences, CW 405, Biological Sciences Centre, University of Alberta, Edmonton, Alberta, T6G 2E9, Canada**Received May 18, 1999; Revised Manuscript Received August 5, 1999*

ABSTRACT: Conjugative transfer of F-like plasmids in *Escherichia coli* is repressed by a plasmid-encoded protein, FinO. FinO blocks the translation of TraJ, a positive activator of transcription of genes required for conjugation. FinO binds a *traJ* antisense RNA, FinP, thereby protecting it from degradation, and catalyzes FinP–*traJ* mRNA hybridization. Interactions between these two RNAs are predicted to block the *traJ* ribosomal binding site. In this paper, we use limited proteolysis, circular dichroism spectroscopy, and an electrophoretic mobility shift assay to map the regions within FinO that are required for interactions with RNA. Our results show that FinO is largely helical, binds to its highest affinity binding site within FinP as a monomer, and contains two distinct RNA binding regions, one of which is localized between residues 26 and 61, and a second which is localized between residues 62 and 186.

The F-plasmid of *Escherichia coli* is transferred to recipient cells via the gene products encoded in the approximately 35 kb transfer (*tra*) region of the plasmid (reviewed in ref 1). The TraJ protein encoded within this region is known to be a positive regulator of transcription of the F *tra* genes from the P_Y promoter located at the start of the transfer region (2). The FinOP (fertility inhibition) system of F and F-like plasmids controls the ability and frequency with which these plasmids are transferred from donor to recipient *E. coli* (3). Control of TraJ expression, and therefore *tra* gene expression and F-plasmid transfer, is mediated by two components comprising the FinOP system, FinP and FinO (3). FinP is an approximately 79 nucleotide RNA molecule which is complementary to the untranslated leader of the *traJ* mRNA (4). This antisense RNA molecule contains two stem–loops which are complementary to the analogous stem–loops in *traJ* mRNA (Figure 1B). FinP is thought to form an RNA/RNA duplex with *traJ* mRNA, occluding the *traJ* ribosome binding site located in the 5' stem–loop of the mRNA and preventing translation of the TraJ protein (5).

The FinO protein encoded by a variety of F-like plasmids (6–8) is a basic, 186 residue protein with a molecular mass of approximately 21.2 kDa (Figure 1A) (9–11). In F, the FinO gene is interrupted by an IS3 insertion. This causes F to be derepressed for transfer (9, 12) and demonstrates the requirement for FinO in promoting the repression of F transfer. FinO stabilizes FinP in vivo, presumably by

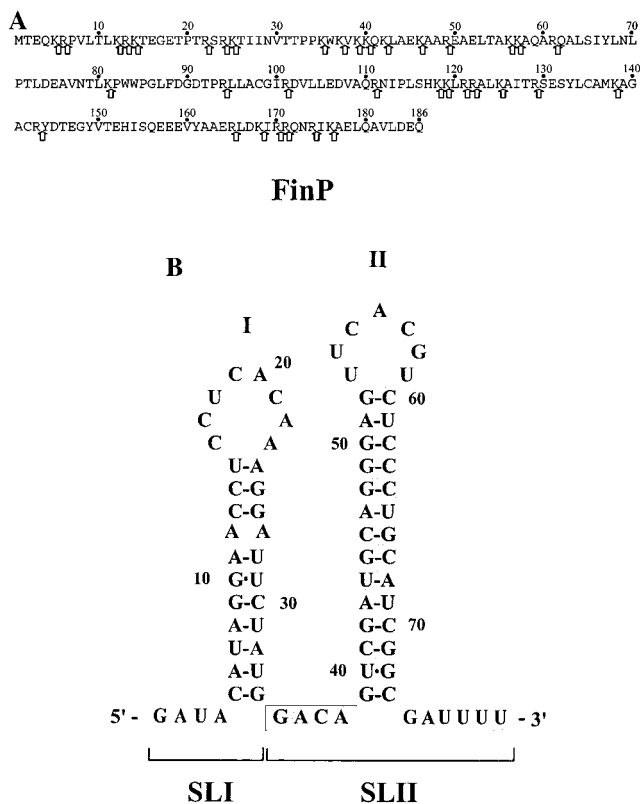


FIGURE 1: Primary sequence of FinO and FinP. (A) The amino acid sequence of FinO encoded by the R6-5 plasmid is displayed using the single-letter code. Arrows indicate the positions of potential trypsin cleavage sites immediately C-terminal to lysine and arginine residues. (B) The nucleotide sequence and secondary structure of FinP are displayed. The stem–loop region (SLII) which is a high-affinity binding site for FinO is highlighted in gray (17).

preventing its degradation by RNase E, thus increasing its in vivo concentration (13, 14). FinO can then bind to both FinP and *traJ* RNA, promoting duplex formation and blocking TraJ translation (11, 15, 16).

[†] Supported by the Alberta Heritage Foundation for Medical Research and MRC (Canada) Grant 11249. J.N.M.G. is an Alberta Heritage Foundation for Medical Research Scholar. M.J.G. was supported by an MRC (Canada) studentship.

* To whom correspondence should be addressed at the Department of Biochemistry, 4-74 Medical Sciences Building, University of Alberta, Edmonton, Alberta, T6G 2H7, Canada. Telephone: 780-492-2136. Fax: 780-492-0886. E-mail: mark.glover@ualberta.ca.

[‡] Department of Biochemistry, University of Alberta.

[§] Department of Biological Sciences, University of Alberta.

Recent biochemical studies have shed light on how FinO selectively binds to both TraJ and FinP RNAs (17). The lack of sequence similarity between these RNAs suggests that FinO does not bind in a sequence-specific manner. Instead, these studies showed that FinO recognizes a specific RNA structure that is common to both FinP and *traJ* RNA. The minimal RNA target appears to be a stem-loop structure with 5' and 3' single-stranded tails. Because of this, FinO derived from one plasmid can repress the transfer of other F-like plasmids (18).

The structural principles that underlie the ability of FinO to interact with RNA are currently unknown. To delimit functionally important regions of FinO, Sandercock and Frost (11) assayed the ability of a variety of FinO deletion mutants to bind RNA, catalyze sense-anti-sense recognition, inhibit cleavage of FinP, and repress F plasmid conjugation. These studies showed that N-terminal fragments of FinO, but not a C-terminal FinO fragment, could specifically bind FinP and *traJ* RNA and catalyze their hybridization in vitro. Although these results suggested that the C-terminal region of FinO does not bind RNA, these studies demonstrated that sequences near the C-terminus are nevertheless required for stabilization of FinP and repression of F transfer in vivo. Motivated by these apparently contradictory results, we have probed the domain structure of FinO using limited proteolysis and circular dichroism spectroscopy and assayed the ability of the isolated domains to interact specifically with FinP. These experiments show that FinO is a largely helical protein which binds to individual RNA binding sites as a monomer. Surprisingly, our results demonstrate that FinO contains two separable regions that each specifically bind FinP RNA. The core of one of these regions is located at the N-terminus of the protein, between residues 26 and 61. The second region is comprised of residues 62–186, and requires sequences at the extreme C-terminus of the protein (residues 175–186) for RNA binding. Taken together with the results of Sandercock and Frost (11), these results suggest that the C-terminal region of FinO blocks RNaseE cleavage of FinP through direct contacts with the RNA.

EXPERIMENTAL PROCEDURES

Construction of pGEX Fusion Plasmids. A clone encoding FinO from pR6-5 as a GST-fusion¹ (pGEX-FO2) was used as a template for constructing the various *finO* derivatives (5). PCR products that contained portions of the *finO* gene were inserted into a GST-fusion vector (pGEX-KG), between a 5' *Bam*HI site and a 3' *Eco*RI site. These GST-fusion constructs were pGEX-FO(1–174), pGEX-FO(62–186), pGEX-FO(62–174), pGEX-FO(62–170), pGEX-FO(26–186), and pGEX-FO(1–61). The upstream primers used to make these constructs were 5FO1 (5'-CCGACGGGATC-CATGACAGAGCAGAAGCGACCG-3'), 5FO62 (5'-C-CGACGGGATCCCAGGCGCTGTCCATTTATCTG-3'), 5FO62, 5FO26 (5'-CCGACGGGATCCACCATCATCAAT-GTCACCACG-3'), and 5FO1, respectively. The downstream primers were 3FO174 (5'-CCGACGGAATTCTTACCGGT-

TCTGGCGGGCGGAT-3'), 3FO186 (5'-CCGACGGAAT-TCTTATTGCTCATCAAGCACGGC-3'), 3FO174, 3FO170 (5'-CCGACGGAATTCTTAGCGGATTTTATCCAGACG-3'), 3FO186, and 3FO61 (5'-CCGACGGAATTCTTATCTG-GCCTGCGCTTTTTT-3'), respectively. The upstream primers contain a *Bam*HI site, and the downstream primers contain an *Eco*RI site. This allowed direct cloning into pGEX-KG.

In Vitro Transcription of Full-Length FinP and FinP SLII RNA. In vitro transcription reactions were carried out as described previously (14). Briefly, FinP was transcribed from pLJ5-13 template DNA (which encodes FinP under the control of a bacteriophage T7 promoter), linearized with *Bam*HI. Runoff in vitro transcription using this template yields FinP with seven additional nucleotides (5'-GGG-GAUC-3') added to the 3' end (14). SLII RNA was transcribed from the synthesized template 5'-AAAATCGC-CGATGCAGGGAGACGTGAACTCCCTGCATCGA-CTGTCTATAGTGAGTCGTATTA-3' and the complementary T7 primer 5'-TAATACGACTCACTATAG-3'. [³²P]-GTP and [³²P]UTP were used for labeling SLII and FinP, respectively. RNA was electrophoresed on an 8 M urea polyacrylamide gel and subsequently purified.

Electrophoretic Mobility Shift Assays (EMSA). For experiments performed with full-length FinP RNA, 7.5 fmol of ³²P-labeled FinP was incubated with increasing concentrations of FinO deletion proteins in separate reactions. RNA and protein were mixed in a total volume of 30 μ L containing 50 mM Tris-HCl (pH 8), 1 mM EDTA, 100 mM NaCl, 3.0 μ g of RNase-free BSA (Pharmacia), 2 mM DTT, 10% glycerol, and 7.6 units of RNaguard (Pharmacia). Reactions were incubated for 30 min at 4 °C. In competition assays, *E. coli* total tRNA (1000-fold molar excess vs FinP) was added to reactions containing FinP RNA and incubated at 4 °C for 5 min before addition of the protein. Reactions were loaded onto a continuously running 5% or 8% nondenaturing polyacrylamide gel and electrophoresed for 1 h at 150 V, 4 °C. Polyacrylamide gels contained Tris-glycine buffer (25 mM Tris, 0.19 M glycine, pH 8–8.3), which was also used as the running buffer. Gels were imaged on Molecular Dynamics storage phosphor screens with a Molecular Dynamics Phosphorimager 445 SI and quantitated using Molecular Dynamics ImageQuANT software.

The apparent equilibrium association constant (K_a) for each FinO-FinP RNA complex was calculated from the equilibrium expression:

$$K_a = \frac{[\text{FinO} \cdot \text{FinP}]}{[\text{FinO}][\text{FinP}]}$$

where [FinO·FinP], [FinO], and [FinP] refer to the equilibrium concentrations of FinO·FinP complex, free FinO, and free FinP, respectively. The ratio of FinO-bound FinP to free FinP for each binding reaction was determined from the ratio of the intensities of the bands corresponding to the bound and free FinP species. Because FinO was in vast molar excess over FinP in all reactions, the total FinO concentration was assumed to be equivalent to [FinO]. K_a values were determined for each binding reaction and averaged for a given titration experiment. Unless otherwise specified, all K_a determinations were obtained from at least three separate titration experiments.

¹ Abbreviations: β ME, β -mercaptoethanol; BSA, bovine serum albumin; CD, circular dichroism; DEPC, diethyl pyrocarbonate; DTT, dithiothreitol; EMSA, electrophoretic mobility shift assay; GST, glutathione S-transferase; PCR, polymerase chain reaction; PAGE, polyacrylamide gel electrophoresis; SL, stem-loop.

EMSA experiments with SLII RNA and FinO and GST-FinO were performed in a similar manner. Each reaction contained 40 μM ^{32}P -SLII RNA and 2.5 μM GST-FinO and/or FinO. Proteins were mixed first and incubated for 30 min at 25 °C followed by another 30 min incubation at 4 °C. SLII was then added, and the samples were incubated for another 30 min at 4 °C. Gel electrophoresis was performed as described above, and the positions of RNA-containing species within the gel were visualized by autoradiography.

Purification of FinO and FinO-Derived Fragments. FinO and its fragments were expressed as glutathione-*S*-transferase (GST) fusions from the pGEX-KG vector (Pharmacia). FinO overexpression plasmids were transformed into *E. coli* DH5 α strains. One liter cultures of these strains were grown in LB + 100 $\mu\text{g}/\text{mL}$ ampicillin at 37 °C. At an OD₆₀₀ of 0.8, the culture was moved to 25 °C and induced with 0.2 mM IPTG. After 5 h of growth, cells were harvested and stored at -70 °C overnight. Cells were resuspended in 50 mL of 50 mM potassium phosphate (pH 6.5), 150 mM NaCl, 1 mM EDTA, 0.1% β ME, 0.1 mg/mL PMSF, 1 $\mu\text{g}/\text{mL}$ pepstatin, 1 $\mu\text{g}/\text{mL}$ leupeptin, and 0.1 mg/mL lysozyme, and the cell solution was mixed for 30 min, at 4 °C, to break down the cell wall. Lysis of cells was completed by brief sonication. The lysate was spun at 30000g to remove insoluble debris, and the cleared lysate was loaded onto a 10 mL glutathione-agarose column (Pharmacia). The column was subsequently washed with a solution of 50 mM Tris-HCl (pH 8.5), 150 mM NaCl, and 1 mM EDTA, and GST-FinO was eluted with the same buffer containing 20 mM reduced glutathione. Fractions containing FinO were pooled (about 25 mL) and were incubated with 17 units of thrombin for ~16 h to cleave GST from FinO. The digestion was stopped by addition of PMSF to a final concentration of 10 $\mu\text{g}/\text{mL}$. FinO was purified from GST by cation exchange chromatography using a 30 mL Fast-SP column (Pharmacia) and a 10 column volume gradient from 0 to 1 M NaCl in a buffer containing 50 mM potassium phosphate (pH 6.5), 1 mM EDTA, and 0.1% β ME. FinO fragments eluted from this column at approximately 400 mM NaCl. Fractions containing purified FinO (determined by polyacrylamide gel electrophoresis) were diluted 3-fold with the 50 mM potassium phosphate (pH 6.5) buffer and were bound to a 1 mL Fast-SP column. Concentrated FinO was eluted from this column with 1–2 mL of 600 mM NaCl, 50 mM potassium phosphate (pH 6.5), 1 mM EDTA, and 0.1% β ME. Protein concentrations were determined by the Bradford assay (BIORAD), which was calibrated for the true molar concentration of each of the protein fragments by amino acid analysis.

Proteolysis. Reactions contained 200 μg (9 nmol) of FinO, 230 mM NaCl, 19 mM potassium phosphate, 11 mM Tris-HCl, 38% glycerol, 1 mM EDTA, 0.1% β ME, and, in some experiments, 410 μg (28 nmol) of SLII RNA, in a total volume of 105 μL . Samples were equilibrated at 25 °C for 30 min. For 25 °C reactions, 4 μL of a 50 $\mu\text{g}/\text{mL}$ stock of trypsin was added to initiate the reactions. For 4 °C reactions, samples were incubated at 4 °C for a further 10 min, and 4 μL of 1 mg/mL trypsin was subsequently added. Five microliter aliquots were taken at various times, and 1 μL of 1 mg/mL PMSF was added to stop the digestion. Samples were analyzed by 15% SDS-PAGE. To identify the various proteolytic fragments, trypsin digests were scaled up to 250 μL . At the desired time point, the reactions were stopped

with 3 μL of 1 mg/mL PMSF. Five microliters of this reaction was analyzed by SDS-PAGE. The molecular masses of the proteolytic fragments in the remainder of the reaction were determined by electrospray mass spectroscopy using a VG Quattro triple quadrupole mass spectrometer. The proteolytic fragments FinO(62–170) and FinO(62–174) (Figure 2A) were first purified prior to mass spectroscopy by HPLC using a Zorbax C8 reversed-phase column. The first four N-terminal amino acids of these fragments were determined using an HP G1005A amino acid sequencing system with routine 3.0 chemistry and biphasic column technology at the Alberta Peptide Institute.

Circular Dichroism Spectroscopy. CD spectroscopy for FinO and FinO-derived fragments was performed at a concentration of approximately 1 mg/mL in a buffer containing 50 mM MES, 150 mM NaCl, 5 mM EDTA, and 1% β ME. Exact protein concentrations were determined by amino acid analysis. CD spectra were determined either in the far-UV (190–255 nm) or in the near-UV (255–320 nm) ranges. Protein solutions were loaded into calibrated 0.02 and 1 cm fused silica cells for the far- and near-UV analysis, respectively. Spectra were recorded on a Jasco J-720 spectropolarimeter (Jasco Inc., Easton, MD) interfaced with an Epson Equity 386/25 computer and controlled by Jasco software. A Lauda water bath (Brinkmann Instruments) was used to control the cell temperature. The spectropolarimeter is routinely calibrated with ammonium *d*-(+)-10-camphor-sulfonate at 290.5 and 192 nm. For the far-UV data, mean molar ellipticity is calculated as the ellipticity per mole of protein, rather than per mole of amino acid residue, to facilitate comparison of the spectra obtained from different FinO fragments. The near-UV data are presented as the mean molar ellipticity per mole of aromatic residues. Each data point is the average of 10 samplings. The helical content for each fragment was estimated by Provencher-Glückner analysis (19).

RESULTS

RNA Binding Protects N- and C-Terminal Regions of FinO from Proteolysis. Limited proteolysis is a powerful tool to map domains of ordered secondary and tertiary structure within proteins. In general, segments of polypeptide chain that are unfolded are cleaved more readily than stably folded segments. We used trypsin to probe the structure of FinO because potential trypsin cleavage sites (lysine and arginine residues) are well dispersed throughout this highly basic protein (Figure 1B). To test for changes in FinO structure upon RNA binding, parallel proteolysis experiments were performed in the presence or absence of SLII RNA, a fragment of FinP that contains a single, high-affinity FinO binding site (17). FinO protein used in these studies was overexpressed in *E. coli* and purified to near-homogeneity. SLII RNA was synthesized by in vitro transcription and purified by denaturing PAGE (Experimental Procedures). Reactions were initiated by addition of trypsin to a solution of FinO or FinO in the presence of SLII RNA (Figure 1B) at a 4:1 molar ratio of SLII to FinO. Aliquots were taken at several time points during the reaction, and the digestion products were analyzed by SDS-PAGE and electrospray mass spectrometry (Figure 2). At 25 °C, FinO was digested within 360 min to two major trypsin-resistant fragments (Figure 2A). We could not separate the two species by

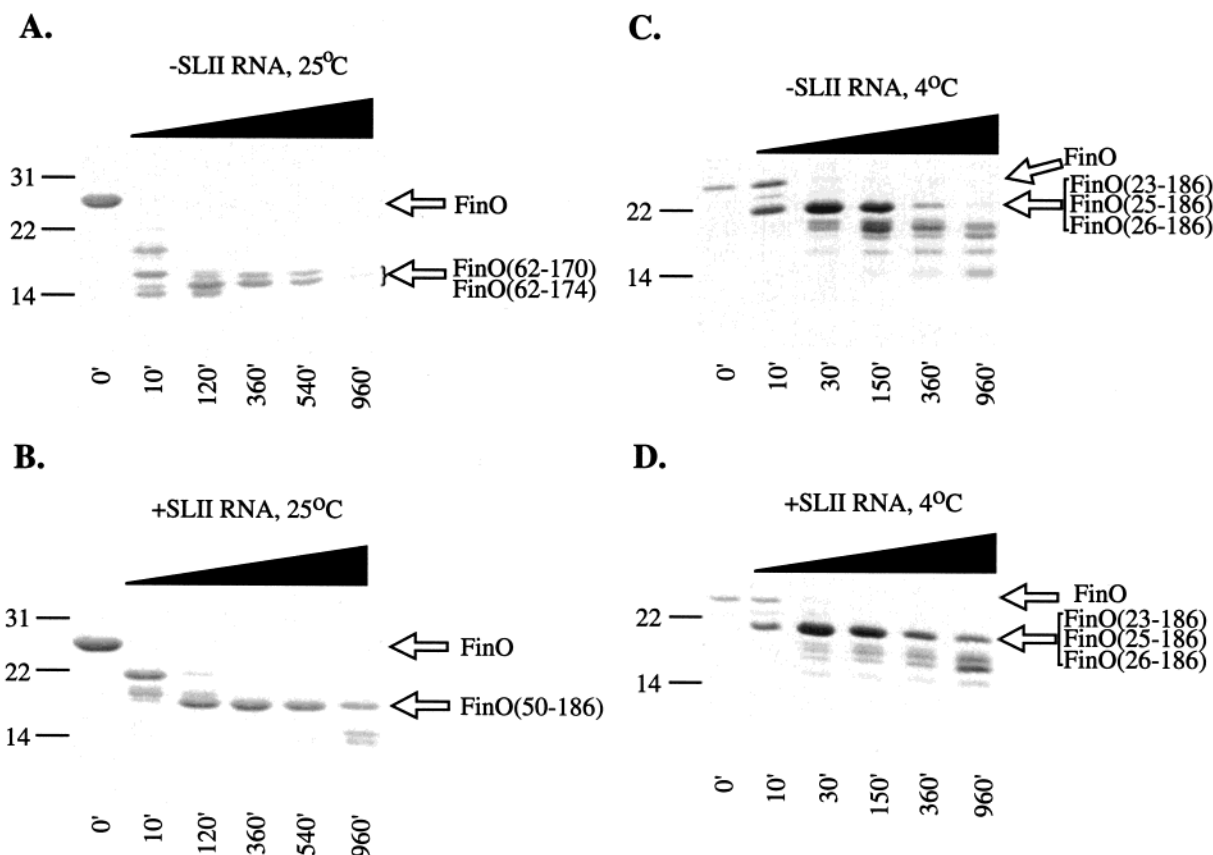


FIGURE 2: N- and C-terminal regions of FinO are protected against trypsin digestion by FinP RNA. Purified FinO was incubated either in the absence (panels A and C) or in the presence of a molar excess of SLII RNA (panels B and D) and digested with trypsin for the indicated times and temperatures. The reaction products were separated by 15% SDS-PAGE and visualized by Coomassie blue staining (see Experimental Procedures). Arrows indicate the positions of migration of FinO and several of the proteolytically derived fragments. Note that in panels C and D FinO(23-186), FinO(25-186), and FinO(26-186) all comigrate.

reversed phase HPLC, and instead the mixture was analyzed by mass spectrometry. Two major peaks were observed: one with a mass of $12\,952 \pm 6.5$ Da, corresponding to a fragment spanning residues 62-174 (predicted mass = 12 959 Da); and the other with a mass of $12\,404 \pm 17$ Da, corresponding to a related fragment spanning residues 62-170 (predicted molecular mass = 12 404 Da). The N-terminus of both fragments was directly determined by N-terminal amino acid sequencing of the mixture (Experimental Procedures). In the presence of SLII, however, a larger FinO fragment was partially protected against proteolytic digestion (Figure 2B). A sample from a 120 min digestion was subjected to mass spectrometric analysis, which revealed the molecular mass for this fragment to be $15\,598 \pm 8$ Da, corresponding to a fragment comprising residues 50-186 (predicted molecular mass = 15 595 Da). Comparison of the earliest digestion time points in Figure 2A and Figure 2B indicates that sequences N-terminal to residue 50 are also stabilized against trypsin digestion when bound to SLII. Similar experiments, performed at 4 °C to slow the digestion, confirm this result (Figure 2C,D). One larger fragment, migrating slightly faster than the 22 kDa molecular mass marker, was stabilized by RNA in these experiments, although, unlike FinO(50-186) at room temperature, this fragment was also somewhat stable in the absence of RNA. Mass spectrometric analysis of a 30 min reaction in the presence of RNA at 4 °C (Figure 2D) revealed that the major proteolytic species are three related fragments that comigrate in SDS-PAGE. The three fragments span residues 23-186 (experimentally determined

molecular mass = $18\,695 \pm 6$ Da, predicted molecular mass = 18 697 Da), 25-186 (experimentally determined molecular mass = $18\,457 \pm 6$ Da, predicted molecular mass = 18 454 Da), and 26-186 (experimentally determined molecular mass = $18\,330 \pm 6$ Da, predicted molecular mass = 18 326 Da). These results suggest that residues 1-61 at the N-terminus and residues 170-186 at the C-terminus of FinO are flexible, relative to the central region (residues 62-170). In complex with SLII RNA, residues 23-61 in the N-terminal region and potential trypsin cleavage sites around residues 170-174 near the C-terminus become more resistant to trypsin digestion, suggesting that these residues directly contact RNA and/or undergo a transition to a proteolytically resistant conformation in response to RNA binding.

Analysis of the Structure of FinO by Circular Dichroism Spectroscopy. To better understand the structures of the N-terminal, central, and C-terminal regions of FinO, we overexpressed and purified fragments of FinO corresponding to a number of the FinO trypsin fragments (Figure 3) and analyzed their structures by circular dichroism spectroscopy (Figure 4). The spectra were all measured under identical conditions to facilitate their comparison. The far-UV spectra of FinO, FinO(62-174), and FinO(62-186) are all very similar, and display double minima near 208 and 220 nm, indicating that all these proteins contain a large proportion of α -helix (Figure 4A). Provencher-Glückner analysis (19) of these spectra indicates that each fragment contains approximately 50% α -helix. In contrast, the far-UV spectrum of the N-terminal region, FinO(1-61), shows a major

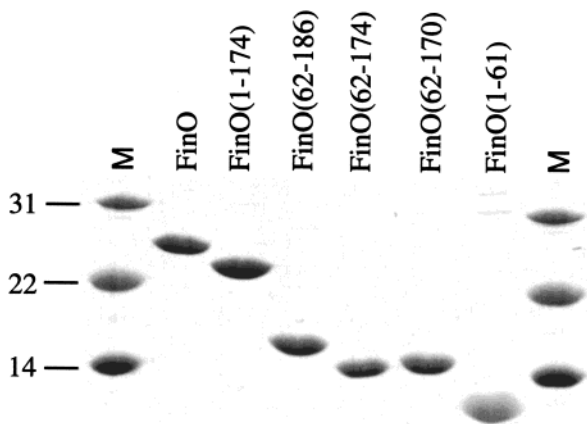


FIGURE 3: Denaturing polyacrylamide gel electrophoresis of purified FinO and FinO-derived fragments. FinO, FinO(62–174), FinO(62–170), FinO(1–174), FinO(62–186), and FinO(1–61) were overexpressed in *E. coli* and purified as described under Experimental Procedures. Approximately 2 μg of each purified protein was analyzed by 15% SDS–PAGE, and visualized by Coomassie blue staining.

minimum near 200 nm and a much smaller minimum near 222 nm, indicative of random coil structure in this isolated fragment and much less helical structure. However, the difference spectrum [FinO – FinO(62–186)] (where the FinO(62–186) spectrum has been scaled to FinO) displays double minima near 208 and 222 nm, indicative of α -helical structure (Figure 4B). Comparison of the FinO(1–61) spectrum and the [FinO – FinO(62–186)] difference spectrum therefore suggests that the 1–61 and 62–186 domains interact in full-length FinO to induce helical structure, most likely in the N-terminal (1–61) region.

Comparison of the far-UV CD spectra of FinO, FinO(62–186), and FinO(62–174) indicates that deletion of either the N- or the C-terminal region does not greatly affect the secondary structure of the central domain. To determine if the N- and C-terminal regions have any effect on the tertiary structure of the central domain, we also measured near-UV CD spectra of these proteins (Figure 4C). Circular dichroism in the near-UV region (255–320 nm) is largely affected by the packing interactions of aromatic residues. Aromatic residues that are packed within a hydrophobic protein core tend to yield complex near-UV spectra with either positive or negative ellipticity. In contrast, protein structures which lack tertiary packing interactions give very little signal in near-UV CD spectra (20). FinO, FinO(62–186), and FinO(62–174) have seven aromatic residues in common, with an additional N-terminal tryptophan in full-length FinO. The similarity in the number of aromatic residues in these fragments allows a comparative analysis of the spectra of these proteins (Figure 4C). The overall pattern and the magnitude of the peaks are very similar for all three proteins, indicating that the packing of the common aromatic residues is similar in all three proteins. Taken together with the far-UV CD results, we can conclude that neither residues 1–61 nor residues 175–186 exert a significant effect on the secondary or tertiary structure of the central domain of FinO (residues 62–174).

The N- and C-Terminal Regions of FinO Each Specifically Bind FinP. Our proteolytic studies suggested that the N-terminal region (residues 1–61) and the C-terminal region

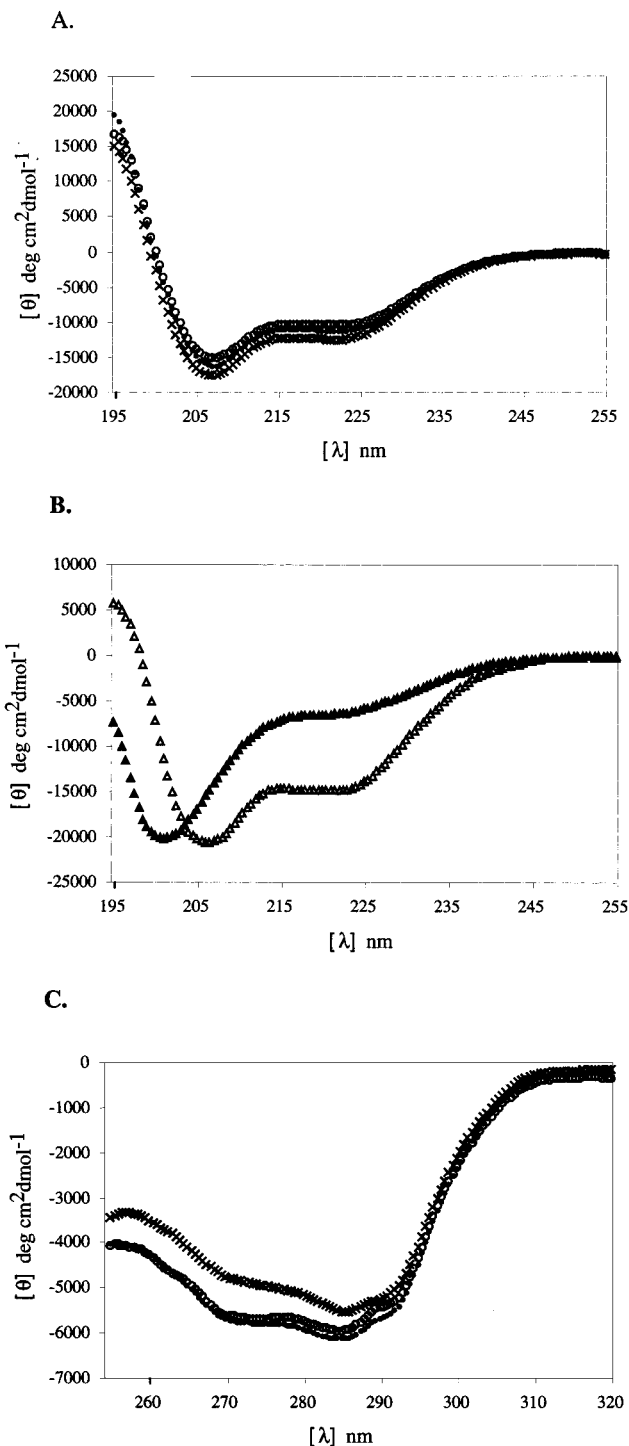


FIGURE 4: Circular dichroism spectroscopy of FinO. (A) The far-UV CD spectra of full-length FinO (+), FinO(62–186) (●), and FinO(62–174) (○) were determined at 4 °C. (B) The far-UV CD spectrum of FinO(1–61) (▲) and the difference spectrum [FinO – FinO(62–186)] (Δ) were determined at 4 °C. (C) The near-UV CD spectra of full-length FinO (+), FinO(62–186) (●), and FinO(62–174) (○) were determined at 4 °C. Mean molar ellipticities were calculated per number of aromatic residues to allow for comparison.

(residues 175–186) contact FinP. To more directly test this hypothesis, we measured the ability of purified FinO and its fragments (Figure 3) to bind FinP RNA in an electrophoretic mobility shift assay (EMSA; see Experimental Procedures). To determine if the observed interactions were specific for FinP, we also performed parallel binding reactions in the

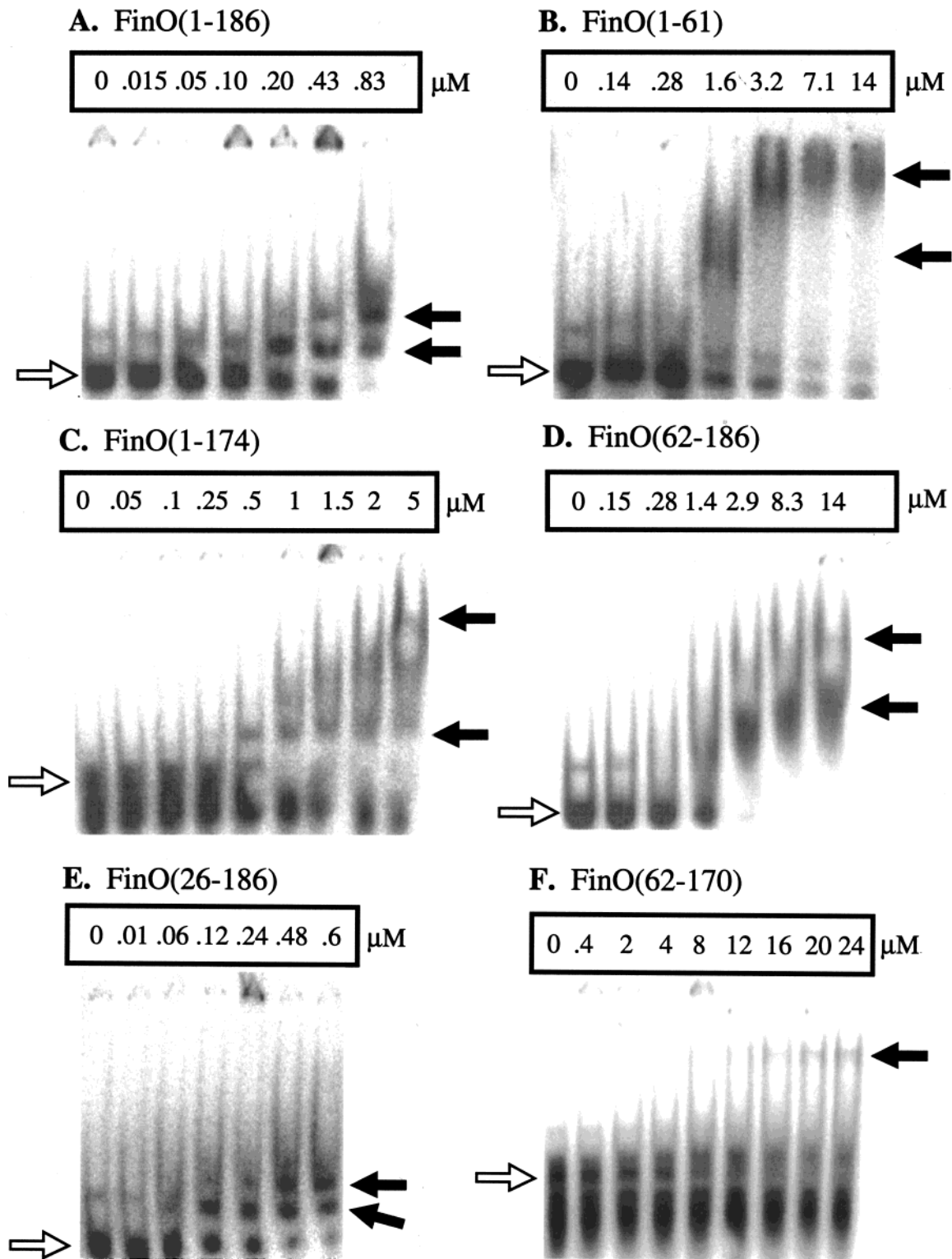


FIGURE 5: Measurement of the ability of FinO deletion proteins to bind FinP RNA by EMSA. In each case, FinO protein or the indicated fragment was incubated with 7.5 fmol of ^{32}P -labeled FinP RNA. Bound (closed arrows) and unbound (open arrows) FinP shown in each gel were resolved by electrophoresis on 5% polyacrylamide gels and visualized by scanning on a phosphorimager. The concentration of protein present in each binding reaction is shown above each lane. In panels A–E, all binding reactions were performed in the presence of a 1000-fold molar excess of total *E. coli* tRNA as nonspecific competitor; in panel F, no competitor was used.

presence of a 1000-fold molar excess of total *E. coli* tRNA as nonspecific competitor. The results of several representative experiments are shown in Figure 5. Each protein fragment that contains either the N-terminal region [FinO (Figure 5A), FinO(1–61) (Figure 5B), or FinO(1–174) (Figure 5C)] or the C-terminal region [FinO (Figure 5A) or FinO(62–186) (Figure 5D)] is able to bind FinP even in the

presence of competitor tRNA, giving rise to several species of reduced mobility relative to free FinP. The presence of multiple retarded species suggests that there are several FinO binding sites in FinP (5, 17). In contrast, fragments lacking both the N- and C-terminal regions [FinO(62–174) (data not shown) and FinO(62–170) (Figure 5F)] bind only weakly to FinP.

Table 1: Apparent K_a of the Various FinO Deletion Proteins in the Presence and Absence of the Nonspecific Competitor *E. coli* tRNA

| FinO fragment | K_a (M^{-1}) | |
|---------------------|-----------------------------|-----------------------------|
| | no competitor ^b | +competitor ^b |
| whole FinO | $(2.0 \pm 0.5) \times 10^7$ | $(5.1 \pm 0.3) \times 10^6$ |
| 1–174 | $(2.7 \pm 1.1) \times 10^6$ | $(1.1 \pm 0.2) \times 10^6$ |
| 26–186 | $(3.2 \pm 0.3) \times 10^7$ | $(7.3 \pm 1.8) \times 10^6$ |
| 62–186 | $(4.2 \pm 1.0) \times 10^6$ | $(8.1 \pm 1.0) \times 10^5$ |
| 1–61 | $(2.1 \pm 0.7) \times 10^6$ | $(1.4 \pm 0.1) \times 10^6$ |
| 62–170 ^a | 1×10^4 | ND ^c |
| 62–174 ^a | 1×10^4 | ND |

^a K_a was estimated due to the inability of FinO deletion protein to bind more than approximately 35–40% of the ³²P-labeled FinP present in a given EMSA except at extremely high protein concentrations.

^b Competitor was *E. coli* total tRNA in a 1000-fold molar excess compared to FinP. ^c ND: not determined.

To quantitate the relative contributions of the N- and C-terminal domains to FinP binding, we calculated the apparent RNA binding constant ($K_{a,app}$) for each fragment in the presence or absence of competitor tRNA (Table 1; see Experimental Procedures). In the absence of tRNA competitor, full-length FinO was found to bind FinP with an apparent binding constant of $2.0 \times 10^7 M^{-1}$, similar to the binding constant determined previously for FinO fused to GST (11, 17). Deletion of residues 1–61 led to a ~5-fold reduction in the binding affinity while deletion of residues 175–186 had a somewhat greater effect, reducing the FinP binding affinity ~10-fold. FinO(62–174) and FinO(62–170), in which both the N- and C-terminal domains have been deleted, bind FinP too weakly to allow accurate quantitation of their binding affinities. However, the affinity of these fragments for FinP appears to be reduced at least 1000-fold compared to full-length FinO. Thus, the central domain, in isolation, plays only a very minor role in RNA binding.

While the binding experiments performed in the presence of competitor indicate that the N- and C-terminal domains both bind FinP specifically, a quantitative analysis of the degree of competition suggests that the specificity of the individual domains may be slightly different. While the apparent affinity of full-length FinO for FinP decreases about 3.9-fold when challenged with tRNA competitor, the apparent affinities of FinO(1–61) and FinO(1–174) for FinP are less affected, decreasing 1.5- and 2.5-fold, respectively, when challenged with the same molar excess of competitor. In contrast, the binding affinity of the C-terminal fragment, FinO(62–186), is more affected by tRNA challenge, decreasing 5.2-fold. Thus, the N-terminal domain may bind FinP somewhat more specifically than the C-terminal domain.

The proteolysis experiments suggested that residues 23–61 were protected against trypsin digestion when bound by RNA but protection of sites closer to the N-terminus could not be detected. To test the role of these more N-terminal residues in RNA binding, we also determined the affinity of purified FinO(26–186) for FinP (Figure 5E). The binding constant of this protein is essentially identical to that of FinO, both in the presence and in the absence of tRNA competitor. Therefore, we conclude the N-terminal RNA binding domain lies within residues 26–61.

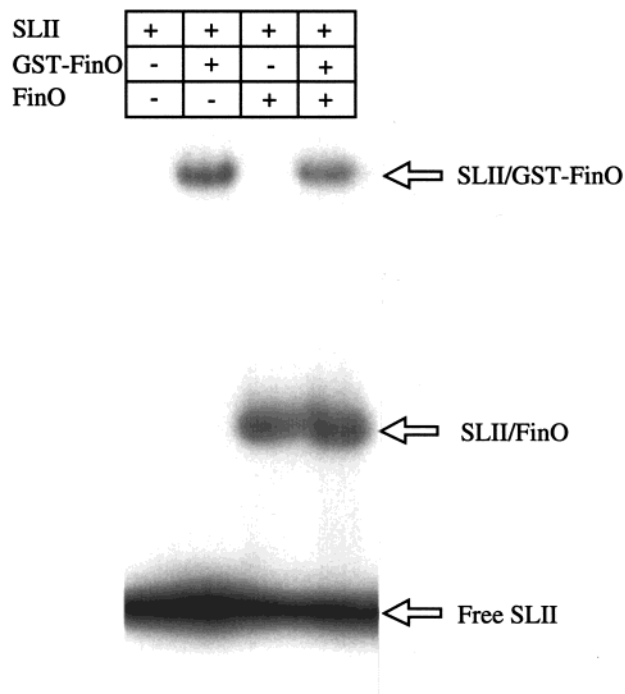


FIGURE 6: EMSA demonstrates that FinO binds FinP as a monomer. ³²P-labeled SLII RNA was incubated with FinO and/or GST-FinO, as indicated at the top of the figure, and the resulting protein–RNA complexes were analyzed by nondenaturing gel electrophoresis as described under Experimental Procedures. Arrows indicate the positions of the SLII/FinO and SLII/GST-FinO complexes, as well as free SLII.

FinO Binds RNA as a Monomer. FinO might facilitate *traJ*–FinP interactions by simply bringing the two RNAs together, initially through protein–protein interactions between two FinO molecules, one bound to TraJ and the other to FinP. To test this hypothesis, we first employed equilibrium analytical ultracentrifugation to probe the oligomeric state of free FinO in solution (data not shown). These experiments indicated that FinO exists primarily as a monomer at concentrations similar to in vivo levels (~1–10 μM).² However, these experiments also demonstrated that FinO aggregates at much higher concentrations (~1 mM), leaving open the possibility that FinO might oligomerize when bound to RNA.

We next used EMSA to determine the oligomeric state of FinO when bound to the single binding site present in SLII RNA (Figure 6). A similar method was first used to show that the bZIP DNA binding protein GCN4 interacts with DNA as a dimer (21). In this experiment, we bound FinO, GST-FinO, or a mixture of these two proteins to SLII and separated the resulting complexes by nondenaturing PAGE (Figure 6). As previously shown (17), GST-FinO binds this RNA to give a single protein–RNA complex with reduced mobility compared to free SLII. Likewise, FinO also binds SLII to give a single protein–RNA complex. Due to the difference in molecular mass between FinO and GST-FinO, the FinO–SLII complex migrates faster than the GST-FinO–SLII complex. To determine the stoichiometry of binding, we premixed GST-FinO and FinO, added SLII, and separated

² M. J. Gubbins and L. S. Frost, unpublished results.

the resulting mixture by nondenaturing PAGE. We reasoned that if FinO binds SLII as a dimer or higher order aggregate, we would observe not only GST-FinO-SLII and FinO-SLII complexes, but also heteromeric GST-FinO-FinO complexes bound to SLII. The heteromeric complexes would be expected to migrate in the EMSA between the positions of the GST-FinO-SLII and FinO-SLII complexes. However, as shown in Figure 6, only GST-FinO-SLII and FinO-SLII complexes are observed. The fact that FinO and GST-FinO both bind FinP with almost identical affinities [$\sim(2-5) \times 10^7 \text{ M}^{-1}$, Table 1 and ref 11] suggests that fusion to GST does not significantly affect the oligomeric state of FinO when bound to RNA. We therefore conclude that, under these conditions, FinO binds the SLII region of FinP as a monomer.

DISCUSSION

Our results indicate that FinO contains two distinct RNA binding regions which can bind RNA independently of one another. One region is located within the N-terminal third of the protein, between residues 26 and 61, while the second region extends from residues 62 to 186. While we have not delimited the precise boundaries of the C-terminal RNA binding region, two lines of evidence suggest that its primary RNA contact surface is located in the vicinity of a cluster of positively charged residues (165–176) near the C-terminus of the protein (Figure 1A). First, FinP binding protects FinO from trypsin cleavage at residues 170 and 174, suggesting that FinP binding sterically blocks access of the protease to this region of FinO. Second, deletion of residues 175–186 from FinO(62–186) almost completely abolishes the ability of this protein to interact with FinP. The similarity of the CD spectra of FinO(62–174) and FinO(62–186) suggests that this is not an indirect effect caused by a conformational change in residues 62–174 upon deletion of residues 175–186 (Figure 4). We have not mapped the precise N-terminal boundary of the C-terminal domain; however, our proteolytic mapping studies suggest that this boundary lies somewhere between residue 62 and the next potential trypsin cleavage site at residue 81 (Figure 1A). Taken together with our results, the previous finding that a 37 amino acid C-terminal fragment of FinO does not bind FinP (11) suggests that, while this region may contain an essential RNA contact surface, it requires the entire 62–186 domain to interact with FinP.

Sandercock and Frost previously showed that residues 161–186 at the C-terminus of FinO are required to protect FinP from digestion by cellular RNases (11). RNase E appears to be the enzyme responsible for FinP degradation in vivo, cleaving FinP at a specific site located within a single-stranded region that links the two stem-loop structures (17). This single-stranded region is also required for high-affinity binding of FinP by FinO (17). It therefore is likely that FinO(62–186) contacts this single-stranded region, and may sterically block cleavage of this strand by RNase E.

Full-length FinO or FinO(26–186), both of which contain the N- and C-terminal RNA binding regions, yield complexes with FinP which have distinct, defined electrophoretic mobilities, giving rise to relatively sharp bands in EMSA (Figure 5). In contrast, the fragments which contain only one of the RNA binding regions form complexes with FinP that

give much more diffuse bands, and retard the RNA to a greater degree than either FinO or FinO(26–186). This behavior may be explained by nonspecific aggregation of FinO(1–61), FinO(1–174), and FinO(62–186) on the RNA. The diffuse nature of the bands observed with these fragments might also indicate that a significant proportion of these complexes dissociate during electrophoresis. These observations suggest that both RNA binding domains are required to form a kinetically stable complex with FinP, compared to fragments containing only one of the RNA binding regions.

Perhaps the most intriguing aspect of FinO function is the ability of the protein to facilitate sense-antisense interactions between FinP and *traJ* mRNA. The ROM protein of ColE1 performs an analogous function, facilitating the recognition of two complementary RNAs, RNAI and RNAII (22). In both the F and ColE1 systems, initial RNA recognition most likely occurs through base-pairing interactions between complementary loops to form “kissing” complexes. While ROM directly interacts with the kissing complex and facilitates its conversion to duplex, FinO instead binds to the individual RNAs (17). How, then, does FinO facilitate FinP-*traJ* mRNA recognition? One mechanism could involve FinO bringing together FinP and *traJ* via protein-protein interactions between FinO molecules bound to separate RNAs which have formed the kissing complex. Our results, however, show that FinO binds an isolated, single RNA target as a monomer. Therefore, if FinO does facilitate FinP-*traJ* mRNA recognition through protein-protein interactions, these interactions must be extremely weak in the absence of both RNA targets. Alternatively, a FinO monomer may stabilize the kissing complex, or FinO-dependent RNA annealing may be facilitated by some other mechanism. For example, FinO might destabilize intramolecular base-pairing within FinP and *traJ* mRNA, allowing complementary base pairs to form between these two RNAs.

FinO bears no sequence similarity to other known RNA binding proteins. While our studies clearly show that there are two separate regions of FinO that contact RNA, we still do not know if these regions form two independent structural domains, or if the two regions come together in the intact protein to form a single contiguous RNA contact surface. High-resolution structural studies of FinO, alone and bound to minimal RNA targets, will be required to answer this question and reveal, at a fundamental level, how this protein recognizes RNA in a structure-specific manner.

ACKNOWLEDGMENT

We are grateful to Les Hicks for assistance with sedimentation equilibrium experiments, Lorne Burke for electrospray mass spectrometry, and Lori Jerome for helpful discussions.

REFERENCES

1. Frost, L. S., Ippen-Ihler, K., and Skurray, R. A. (1994) *Microbiol. Rev.* 58, 162–210.
2. Cuzzo, M., and Silverman, P. M. (1986) *J. Biol. Chem.* 261, 5175–5179.
3. Finnegan, D., and Willetts, N. (1972) *Mol. Gen. Genet.* 119, 57–66.
4. Mullineaux, P., and Willetts, N. (1985) *Basic Life Sci.* 30, 605–614.
5. van Biesen, T., and Frost, L. S. (1994) *Mol. Microbiol.* 14, 427–436.

6. Cram, D. S., Loh, S. M., Cheah, K. C., and Skurray, R. A. (1991) *Gene* 104, 85–90.
7. McIntyre, S. A., and Dempsey, W. B. (1987) *Nucleic Acids Res.* 15, 2029–2042.
8. van Biesen, T., and Frost, L. S. (1992) *Mol. Microbiol.* 6, 771–780.
9. Yoshioka, Y., Ohtsubo, H., and Ohtsubo, E. (1987) *J. Bacteriol.* 169, 619–623.
10. Yoshioka, Y., Fujita, Y., and Ohtsubo, E. (1990) *J. Mol. Biol.* 214, 39–53.
11. Sandercock, J. R., and Frost, L. S. (1998) *Mol. Gen. Genet.* 259, 622–629.
12. Cheah, K. C., and Skurray, R. (1986) *J. Gen. Microbiol.* 132, 3269–3275.
13. Lee, S. H., Frost, L. S., and Paranchych, W. (1992) *Mol. Gen. Genet.* 235, 131–139.
14. Jerome, L. J., van Biesen, T., and Frost, L. S. (1999) *J. Mol. Biol.* 285, 1457–1473.
15. van Biesen, T., Soderbom, F., Wagner, E. G., and Frost, L. S. (1993) *Mol. Microbiol.* 10, 35–43.
16. Koraimann, G., Teferle, K., Markolin, G., Woger, W., and Hogenauer, G. (1996) *Mol. Microbiol.* 21, 811–821.
17. Jerome, L. J., and Frost, L. S. (1999) *J. Biol. Chem.* 274, 10356–10362.
18. Willetts, N., and Maule, J. (1986) *Genet. Res.* 47, 1–11.
19. Provencher, S. W., and Glöckner, J. (1981) *Biochemistry* 20, 33–37.
20. Woody, R. W. (1995) *Methods Enzymol.* 246, 34–71.
21. Hope, I. A., and Struhl, K. (1987) *EMBO J.* 6, 2781–2784.
22. Predki, P. F., Nayak, L. M., Gottlieb, M. B., and Regan, L. (1995) *Cell* 80, 41–50.

BI9911482